Journal of Hazardous Materials 170 (2009) 763–770

Contents lists available at ScienceDirect

Journal of Hazardous Materials

journal homepage: www.elsevier.com/locate/jhazmat

Adsorption kinetics and performance of packed bed adsorber for phenol removal using activated carbon from dates' stones

Yahia A. Alhamed

King Abdulaziz University, Faculty of Engineering, Department of Chemical and Materials Engineering, P.O. Box 80204, Jeddah 21589, Saudi Arabia

ARTICLE INFO

Article history:
Received 8 January 2009
Received in revised form 2 May 2009
Accepted 5 May 2009
Available online 14 May 2009

Keywords:
Phenol
Dates' stones
Activated carbon
Packed bed
Breakthrough
Mass transfer

ABSTRACT

Kinetic studies of phenol adsorption on activated carbon (AC) produced from waste dates' stone (DS) were performed using four different AC particle sizes (1.47, 0.8, 0.45 and 0.225 mm) and initial concentration of phenol of 200 and 400 ppm. Breakthrough data for phenol removal using a packed bed of AC produced from DS were collected over a wide range of operating conditions: bed height = 5, 10, 15, 20, and 25 cm, initial phenol concentration = 50, 100 and 150 ppm, flow rate = 23.3–141.5 ml/min and particle size = 0.45, 0.8, and 1.50 mm. It was found that adsorption kinetics of phenol can be very well represented by the pseudo-second order equation. The initial rate of adsorption (h) predicted from the pseudo-second order model, decreased with increasing particle diameter (d_p) as a result of higher interfacial surface area provided by particles with smaller d_p. The obtained breakthrough curves were very well fitted using an axial dispersion model (correlation coefficient of 0.997 or better), which enabled the determination of the axial dispersion coefficient and Peclet number (Pe). Additionally, breakthrough data were analyzed using the Equivalent Length of Unused Bed (LUB) approach. Defining the Fractional Equivalent Length of Unused Bed (FLUB) as LUB divided by the bed height it was found that FLUB can be correlated with Pe with fairly good accuracy using the relation: $\text{FLUB} = e^{-0.0713(Pe)}$ for the whole range of experimental parameters explored. It was also shown that the film mass transfer coefficient obtained from the analysis of breakthrough curves for small particle size and short bed at applicable conditions agreed fairly well with that obtained from mass transfer correlation available in literature.

1. Introduction

It has been widely acknowledged the importance of agricultural waste as a cheap source for production of activated carbon, which can be used for removal of various pollutants such as phenols and dyes from wastewater streams. Literatures on this subject included agricultural wastes such as dates' stones [1–6], corn cob [7–9], coconuts shells, nuts shells and nuts stones [10–18], oil palm stones and shells [19–21], apple pulp [22,23], chickpea husks [24], rice straw and lignin [25], and others [26–29]. All these efforts are driven by more stringent pollution control regulations and the need for exploring cheap and renewable raw materials for production of AC. Saudi Arabia produces about 830,000 tons of dates annually [30], which can yield a minimum of 83,000 metric tons of dates' stones. A reasonable fraction of this quantity can be reclaimed easily from dates' processing plants and can be used as a raw material for production of activated carbon.

One of the most hazardous polluting materials to the environment is phenol, which can exert negative effects on different biological processes and their presence even at low concentrations can cause unpleasant taste and odor of drinking water and can be an obstacle to the use (and/or) reuse of wastewater. Industrial sources of environmental contaminants such as oil refineries, coal gasification sites, and petrochemical units generate large quantities of phenols [31].

Adsorption by activated carbons is the best and most frequently used method for phenols removal from wastewaters [31]. Our previous studies [5,6] have shown that a high yield of AC with good adsorption capacity for phenol adsorption could be obtained from dates' stones by chemical activation method.

Previous studies [1–6] on the production of AC from dates' stones were concentrated mostly on the development of the high quality AC. They did not consider the detailed studies of the adsorption process parameters or the kinetics of phenol adsorption or its performance in packed bed absorbers.

Therefore, the objective of this study is to investigate the kinetics of phenol adsorption on AC produced from dates' stones and further explore in detail the performance of the AC in phenol adsorption in packed bed adsorber aiming at collecting information necessary for industrial scale applications of such process.

2. Materials and methods

Details of the preparation of AC by the chemical activation method were reported earlier [5]. In general, the AC preparation

E-mail address: yhamed@kau.edu.sa.

0304-3894/$ – see front matter © 2009 Elsevier B.V. All rights reserved.
doi:10.1016/j.jhazmat.2009.05.002

Table 1
Properties of activated carbon produced from dates' stones [5].

Characteristic	Value	Units
Bulk density	0.74	g/cm^3
Total pore volume	0.456	cm^3/g
Micropore volume	0.355	cm^3/g
Bed porosity	0.427	Dimensionless
Average pore diameter	1.29	nm
BET surface area	951	m^2/g
Freundlich equation parameters	k = 24.6	(mg/g)(l/mg)$^{1/n}$
	n = 2.74	
Langmuir isotherm parameters	q_m = 111.5	mg/g
	K_L = 0.139	l/mg

Freundlich equation $X = kC_e^{1/n}$, Langmuir isotherm $q_e = q_m\ K_L C_e/1 + K_L C_e$

Table 2
Packed bed characteristics and physical properties.

Characteristic	Value	Units
Bed height	5, 10, 20 and 25	cm
Flow rate	23–141	ml/min
Phenol initial conc.	50, 100 and 150	ppm
GAC particle diameter	0.45, 0.8 and 1.47	mm
Bed diameter	11	mm
Liquid viscosity	0.5	g/cm min
Diffusivity of phenol	1.0×10^{-5}	cm^2/s
Water density	1.00	g/cm^3

passes through the following steps: the procedure starts by grinding clean dry (DS) using a disk mill to obtain material with an average particle size of 1.71 mm. DS were impregnated with $ZnCl_2$ water solutions using the ratio of $ZnCl_2$:DS = 0.5. The impregnation was followed by carbonization at 700 °C for 3 h in a cylindrical stainless steel tube. Obtained AC lumps were washed with diluted HCl (3 wt.%) and followed by washing with distilled water till wash is free of chloride ions. Then the AC was dried overnight at 110 °C in a vacuum oven.

2.1. Activated carbon characterization

Characteristics of the AC used in this study were reported in a previous study [5] and it is summarized in Table 1. A Nova 2200e (Quantachrome Instrument USA) along with a NOVAWin2 (Quantachrome Instrument) data analysis software [32] was used for measurements the BET surface areas (SAs), micropore volumes (V_{mic}), mesopore volumes (V_{mes}), and pore size distribution using nitrogen adsorption at −196 °C.

Surface areas and micropore volumes were determined from the application of the BET equation to the nitrogen adsorption data. The total pore volume (V_t) was determined from the amount of N_2 adsorbed at relative pressure of 0.95.

Pore size distribution was calculated by fitting the nitrogen adsorption data using Nonlinear Density Function Theory (NLDFT) assuming a cylindrical pore model. NOVAWin2 software was used to perform these calculations [32,33].

2.2. Adsorption kinetic studies

AC samples were sieved to obtain four different fractions, with average particle sizes of 1.47, 0.8, 0.45 and 0.225 mm. All fractions were degassed in a vacuum oven at 120 °C for 1.5 h. 1.0 g AC of a given fraction was added to 250 ml solution of phenol in water placed in 500 ml caped conical flask. The initial concentration of phenol (C_0) was 200 or 400 ppm. The sample was kept in a shaker at room temperature (22 ± 1 °C) throughout the experiment. All experiments were performed at 200 rpm. The change of phenol concentration with time was followed by withdrawing 1 ml samples at predetermined time intervals using hypodermic syringe fitted with 2 μm sintered steel filter. The concentration of phenol was determined at λ = 268 nm using a Genysis10 UV/VIS spectrophotometer, which was previously calibrated.

2.3. Packed bed adsorption experiments

A Plexiglass cylindrical tube having 11 mm internal diameter and 50 cm height was used to construct the adsorption column. The column was packed with the desired amount of AC to obtain the desired bed height. The bed was held in place between two plugs of glass wool. The glass wool in the lower part of the column was supported by a stainless steel mesh. Glass beads of 5 cm height on the top of the AC layer served as a calming bed section to facilitate a uniform flow throughout the bed cross-section. The phenol solution was fed continuously to the column in a downward flow mode using Masterflex L/S pump Model 77250-62. The change of phenol concentration in the column effluent was determined following the same method mentioned above. The column was kept at room temperature (22 ± 1 °C). The range of variables investigated and packed bed characteristics is summarized in Table 2.

3. Results and discussion

3.1. Phenol adsorption kinetics

3.1.1. Pseudo-first order and pseudo-second order kinetic models

The basic assumption made in deriving the pseudo-first order and pseudo-second order kinetic models is that the adsorption is a pseudo-chemical reaction process. For first and second order kinetics [34–38], the rates are given by Eqs. (1) and (2), respectively:

$$\frac{dq}{dt} = k_1(q_e - q) \tag{1}$$

$$\frac{dq}{dt} = k_2(q_e - q)^2 \tag{2}$$

where q_e and q are the amounts of phenol adsorbed at equilibrium and at time t (min) in mg/g AC and k_1 (min^{-1}) and k_2 (g/mg min) are the pseudo-first order and pseudo-second order rate constants, respectively. The analytical solution for the above equations at initial condition $t = 0$, $q = 0$, is given by:

$$q = q_e(1 - e^{-k_1 t}) \tag{3}$$

$$q = \frac{q_e^2 k_2 t}{(1 + q_e k_2 t)} \tag{4}$$

Eqs. (3) and (4) can be transformed into the linear forms as shown below:

$$\ln(q_e - q) = \ln(q_e) - k_1 t \tag{5}$$

$$\frac{t}{q} = \frac{1}{k_2 q^2} + \frac{t}{q_e} \tag{6}$$

If the adsorption follows the pseudo-first order rate equation, a plot of $\ln(q_e - q)$ against time t should give a straight line. Similarly, t/q should change linearly with time t if the adsorption process obeys the pseudo-second order rate equation and the initial adsorption rate, $dq/dt = h$ at $t \to 0$ is given by $q_e^2 k_2$ [35]:

The data of the adsorption kinetic of phenol was collected for four different average particle diameters (d_p), two initial concentrations of phenol (C_0 = 200 and 400 ppm) and two AC dosage (1.0 and 0.5 g). The obtained data were fitted using both pseudo-first order (Eq. (3)) and pseudo-second order (Eq. (4)) models. Nonlinear regression software (Polymath) was used to determine models parameters (q_e, k_1, k_2 and h) and relevant statistical indicators such as correlation coefficient (R^2) and the mean squared error (MSE).

Table 3
Fitting parameters for the first order and pseudo-second order adsorption kinetics obtained from nonlinear regression.

Exp. no.	d_p (mm)	Initial conc. (ppm)	First order adsorption model				Second order adsorption model				
			q_e (mg/g)	k_1 (min^{-1})	R^2	MSE	q_e (mg/g)	k_2 (g/mg min)	R^2	MSE	h (mg/g min)
1	0.225	200	48.36	0.0613	0.9999	0.022	48.49	0.02588	0.99995	0.0163	60.85
2	0.45	200	48.11	0.0415	0.9992	0.252	48.76	0.00448	0.99999	0.0045	10.65
3	0.45	400	88.8	0.0456	0.9978	2.16	90.3	0.00207	0.9998	0.2004	16.88
4	0.8	200	47.69	0.0322	0.9978	0.719	48.95	0.00209	0.99987	0.0406	5.01
5	1.5	200	46.13	0.0189	0.9861	4.161	48.75	0.00074	0.99997	0.0085	1.76
6	1.5	400	83.8	0.0119	0.9700	26.5	90.4	0.00022	0.99870	1.111	1.80
7[a]	0.45[a]	200	82.2	0.0286	0.9924	6.41	85.4	0.00080	0.99984	0.135	5.83

Volume of solution = 0.25 l, activated carbon dose = 1.0 g, rate of mixing = 200 rpm. MSE = mean squared error = $(1/n)\sum_{i=1}^{n} e_i^2$, where e is the error.
[a] Activated carbon dose = 0.5 g.

Usually a model with smaller MSE and R^2 closer to unity represents the data more accurately than a model with larger MSE and R^2 lower than 1. Comparing the statistical indicators (R^2 and MSE) reported in Table 3 for the two models, it is clear that the pseudo-second order model fits the experimental data much better than the pseudo-first order model for the four d_p investigated and the two initial concentrations of phenol. Also, the predicted values of q_e using the pseudo-second order model are very close to theoretical values (48.7 and 97.0 mg/g for phenol initial concentration of 200 and 400 ppm, respectively) calculated using Freundlich parameters reported in Table 1. Figs. 1 and 2 compare models predictions (solid lines) with experimental values (points) using first order and pseudo-second order models, respectively, for different d_p. Again, it is clear from these figures that better model predictions (solid lines) are obtained using the pseudo-second order model.

At early stage, the adsorption process is controlled by external film diffusion of phenol to the external surface of the AC particles [39], therefore it is expected that an increase in the initial rate of adsorption (h) will be obtained when decreasing d_p or increasing the AC dose for the same C_0 and solution volume. The data presented in Table 3 confirm this dependence of h on d_p and AC dosage where for a given C_0, h decrease with increasing d_p and decreasing AC dose. Ho and McKay [40] reported similar effect of d_p on h for the adsorption of AR114 (Erionel RED RS) on baggase pith. Table 3 also shows that at a given d_p, k_2 decreased with increasing initial concentration of phenol. In this respect our data agrees with many studies for phenol/AC systems [40,41] and other systems [36,42]. For examples Mohd Din et al. [41] reported a value of k_2 = 0.00013 g/mg min compared to 0.00022 g/mg min for the same C_0 (400 ppm) and using AC dosage of 1.0 g/l compared to 2 g/l used in this study.

3.1.2. Intraparticle diffusion model

The adsorption of a solute from a liquid to the surface of a solid adsorbent is solely controlled by intraparticle diffusion when the film diffusion resistance is negligible. The intraparticle diffusion model can be derived from Fick's second law assuming that the intraparticle diffusivity D is constant and the uptake of sorbate by the adsorbent is small relative to the total quantity of sorbate present in the solution. The mathematical expression thus obtained for the intraparticle diffusion model is [34–36]:

$$q = k_p t^{0.5} + I \tag{7}$$

where k_p (mg/g $min^{0.5}$) is defined as the intraparticle diffusion rate constant and I (mg/g) is a constant that gives an idea about the thickness of the boundary layer. A value of I close to zero indicates that diffusion is the only controlling step of the adsorption process [34]. k_p is related to the intraparticle diffusivity (D) as follows:

$$k_p = \left(\frac{3q_e}{d_p}\right)\sqrt{\frac{D}{\pi}} \tag{8}$$

where d_p is the particle diameter. A plot of q versus the square root of time ($t^{0.5}$) should yield a straight line passing through the origin if the adsorption process controlled by intraparticle diffusion and the slope of the straight line is equal to k_p.

The phenol adsorption data were plotted according to Eq. (7) for different particle sizes as shown in Fig. 3. As seen from this figure, the plots were not linear over the whole time range, implying

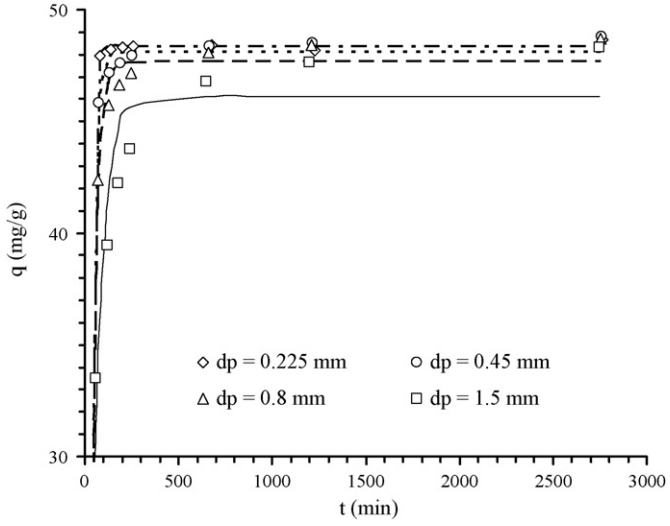

Fig. 1. Fitting of the pseudo-first order model for adsorption of phenol on AC produced from dates' stones. Weight of AC = 1.0 g AC, initial concentration of phenol = 200 ppm. Volume of phenol solution = 250 ml.

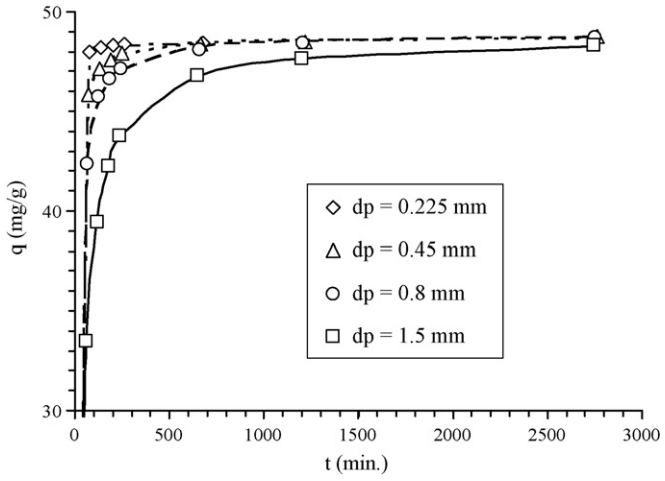

Fig. 2. Fitting of the pseudo-second order model for adsorption of phenol on AC produced from dates' stones. Weight of AC = 1.0 g AC, initial concentration of phenol = 200 ppm. Volume of phenol solution = 250 ml.

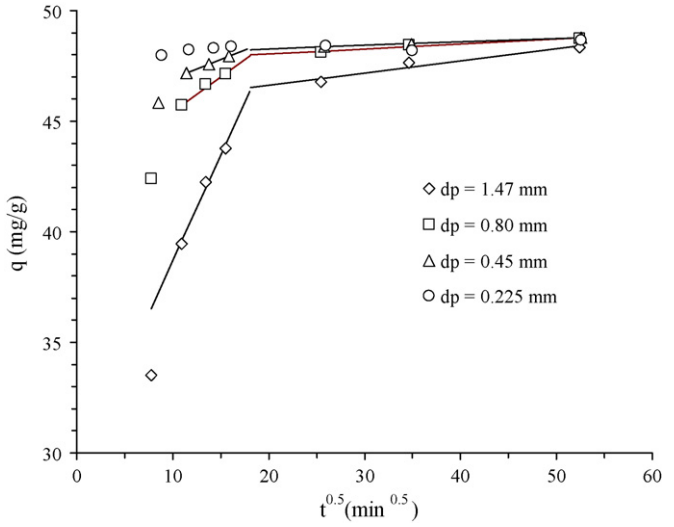

Fig. 3. Plot of the intraparticle diffusion model for adsorption of phenol on AC produced from dates' stones. Weight of AC = 1.0 g AC and initial concentration of phenol = 200 ppm. Volume of phenol solution = 250 ml.

that more than one process affected the adsorption. Such behavior is not unique to our data and it has been reported by many investigators [35,36,39,41–43]. It has been pointed out by Hameed and Rahman [39] that the multiple nature observed in the intraparticle diffusion plot suggests that intraparticle diffusion may not be the only controlling mechanism. Besides, external mass transfer of phenol molecules onto sorbent particles is also significant in the sorption process, especially at the initial reaction period. Fig. 3 shows that for adsorption times below 60 min a fast uptake of phenol is obtained due to adsorption on the external surface area and macropores close to the external surface of the particle. The approach to equilibrium in this region was 67, 87, 94 and 98% for d_p = 0.147, 0.08, 0.045 and 0.0225 cm, respectively. It is clear that the approach to equilibrium is much faster for small d_p due higher interracial surface area available and lower intraparticle diffusion resistance. This fast uptake region is followed by two distinct linear regions that are most likely associated with slow diffusion in the porous structure of AC [36,41,43]. Each linear segment of the curves shown in Fig. 3 was fitted using Eq. (7) by linear regression. The calculated constants (k_p and I) are summarized in Table 4 along with R^2. Also intraparticle diffusivities (D) calculated using Eq. (8) are reported in Table 4. It is clear from this table that I is not zero for the first linear segment of q versus $t^{0.5}$ curve thus indicating a significant resistance due to film (boundary layer) diffusion [39]. An increase in I with decreasing d_p is evident and it may be attributed to lower Reynolds's of smaller particles which in turn lead to higher film diffusion resistance.

Also it can be seen from Table 4 that as d_p decreases from 0.147 to 0.045 cm, D decreases sharply from 30.3557 to 0.0888×10^{-7} cm^2/min and from 4.022 to 0.0108×10^{-7} cm^2/min for the first and second segments, respectively. Kumar et al. [43] reported D values in the order of 10^{-7} cm^2/min for adsorption of phenol by AC (C_0 = 200 ppm and d_p = 0.536 mm) compared to 0.0888×10^{-7} cm^2/min obtained in this study under similar conditions (d_p = 0.47 mm and C_0 = 200 ppm). The lower D obtained is attributed to fact that AC used in this study is highly microporous (see Table 1 and Ref. [5]) and it has a much smaller average pore size (1.29 compared to 5 nm) compared to that used by Kumar et al. [43] which is essentially mesoporous. Such small pore sizes are comparable to the diameter of the phenol molecule which extremely restricts the diffusion of phenol into the micropores (first part of the curve) and ultra micropores (second part of the curve) of the AC. Under these conditions restricted diffusion takes place and very low diffusivities are ought to be obtained as evident in Table 4.

3.2. Modeling phenol adsorption in packed bed adsorber

3.2.1. Axial dispersion model

Modeling of breakthrough curves was achieved by assuming a dispersed plug flow model with an axial dispersion coefficient D_L. This model is described by the differential mass balance equation given below [44]:

$$v\frac{\partial(C)}{\partial z} - D_L\frac{\partial^2 C}{\partial z^2} + \frac{\partial C}{\partial t} + \left(\frac{1-\varepsilon}{\varepsilon}\right)\frac{\partial q}{\partial t} = 0 \quad (9)$$

where v is the interstitial velocity of the carrier fluid, C and q the phenol concentration in the mobile and stationary phase, respectively, z the distance from the inlet of the column, ε the void fraction of the bed and t is the operating time. The assumptions based on which the above equation is derived are: constant temperature and flow rate with position inside the column, no chemical reactions occur in the column; only mass transfer by convection is important and negligible radial dispersion. For a long fixed bed, initially free of solute and with a constant inlet concentration, C_0, the solution of Eq. (9) is [45]:

$$\frac{C}{C_0} = \frac{1}{2}\left\{1 + \mathrm{erf}\left[\left(\frac{vL}{4D_L}\right)\frac{V - V_{min}}{(VV_{min})^{1/2}}\right]\right\} \quad (10)$$

where erf(x) is the error function of x, V the total volume referred to the unit transversal area of the void bed. V_{min} is the minimum volume to saturate the bed per unit transversal area and L is the bed length. The model parameters, D_L and V_{min}, for the adsorption of phenol on AC stones were determined by fitting the experimental data to Eq. (10) using TABLECURVE® program. Peclet number (Pe) was calculated using the estimated dispersion coefficient D_L from Eq. (10) according to the relation:

$$Pe = \frac{vL}{D_L} \quad (11)$$

Eq. (10) was used to fit the experimental breakthrough data. Experimental breakthrough curves (points) and fitting to Eq. (10) (lines) at different conditions are presented in Fig. 4 through 7. A summary of the estimated model parameters (D_L and V_{min}) and other relevant parameters for all breakthrough experiments performed are given in Table 5. It is observed from Table 5 that the correlation coefficient, R^2, was always higher than 0.996 indicating that Eq. (10) can be used to describe the breakthrough data with good accuracy. Figs. 4 and 5 show the effect of flow rate (bed height of 25 cm) and the effect of bed height (flow rate of 23.3 ml/min)

Table 4
Fitting parameters for intraparticle diffusion model for different particle sizes.

d_p (cm)	First linear part of the curve				Second linear part of the curve			
	k_p (mg/g min$^{0.5}$)	I (mg/g)	R^2	D ($\times 10^7$ cm^2/min)	k_p (mg/g min$^{0.5}$)	I (mg/g)	R^2	D ($\times 10^7$ cm^2/min)
0.147	0.9557	29.131	0.986	30.3557	0.0546	45.53	0.941	4.02201
0.08	0.3169	42.237	0.986	0.94938	0.0221	47.591	0.948	0.07251
0.045	0.1723	45.195	0.999	0.08880	0.0157	47.954	0.999	0.01081
0.0225	0.0343	47.81	0.9896	0.00088	0.0116	47.971	0.486	0.00023

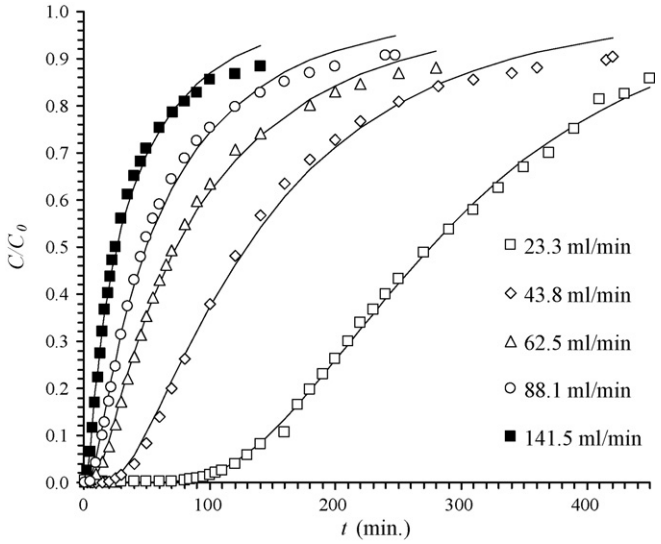

Fig. 4. Effect of flow rate at $L = 25$ cm on breakthrough curves for phenol removal by AC from dates' stones. Particle diameter = 0.8 mm and initial concentration of phenol = 150 ppm.

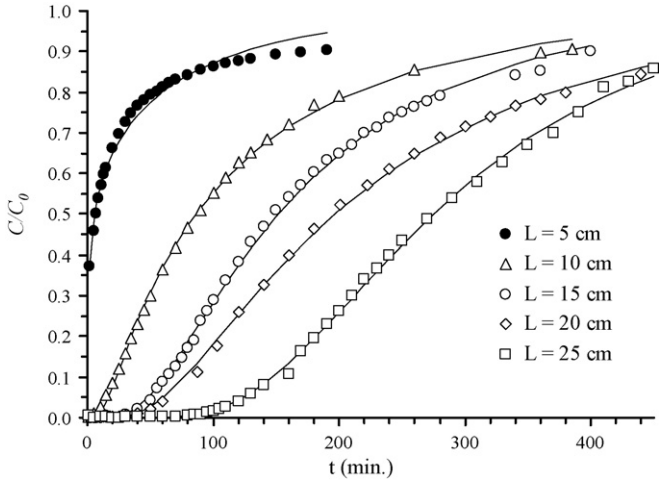

Fig. 5. Effect of flow bed height (L) at a flow rate of 23.3 ml/min on breakthrough curves for phenol removal by AC from dates' stones. Particle diameter = 0.8 mm and initial concentration of phenol = 150 ppm.

on the obtained breakthrough curves, respectively. It is evident from these figures that Eq. (10) fits the experimental data very well especially for long bed and low flow rate. Some deviations are observed at high operating times especially for short beds and at high flow rates. It was assumed that the system can be treated as dispersed plug flow; this assumption seems to be violated under above mentioned conditions due the shift in controlling the mechanisms. Usually for short beds and high flow rates film diffusion is the controlling mechanism at very short operating times [46]. At high operating times it is plausible to say that most of the AC particles are saturated with the adsorbate and the access to the smallest pores closer to the center of the particle becomes slower and thus pore diffusion becomes the controlling mechanism. Even otherwise, Eq. (10) still could be used to describe the system for breakthroughs up to 80% removal of phenol.

The effect of initial concentration of phenol and particle size on breakthrough curves is shown in Figs. 6 and 7, respectively. Eq. (10) fitted the breakthrough data (Table 5) for the three concentrations explored with R^2 equal to 0.997 or higher. On the other hand, the experiments with different particle sizes (Fig. 7) showed that a decrease in particle size improves the performance of the adsorption column where Pe increases from 0.674 for $d_p = 0.8$ mm to 6.309 when the particle diameter is 0.45 mm. As particle diameter decreases the packed bed adsorber approaches plug flow behavior due to lower dispersion. Although small particles provide better usage of the bed, it is not of practical application due to high pressure drop in the packed bed.

3.2.2. Equivalent Length of Unused Bed (LUB)

The dynamic capacity of the AC (W_b) is the amount of phenol adsorbed on the AC at the breakpoint, in mg of phenol per gram of AC and can be calculated from knowing the breakthrough time (t_b) using the following expression [47]:

$$W_b = \frac{t_b Q(C_0 - C)}{m} \quad (12)$$

where C and C_0 are the outlet concentration of phenol at breakthrough time and inlet phenol concentration, respectively, Q is the flow rate of the phenol aqueous solution and m is the mass of AC. Apart from the breakthrough time of a bed of specified height, other

Table 5
Summary of breakthrough experiments.

Experimental conditions				FLUB	Model parameters			
Q (ml/min)	L (cm)	C_0 (ppm)	d_p (mm)		D_L (cm²/min)	V_{min} (cm³/cm²)	R^2	Pe
23.9	5	150	1.47	1.000	2,096	147.8	0.983	0.140
42.6	5	150	1.47	1.000	19,867	29.1	0.919	0.026
43.8	10	150	0.80	0.923	1,601	1445.1	0.997	0.674
62.5	15	150	0.80	0.985	2,515	2479.1	0.997	0.918
43.8	10	100	0.80	0.977	1,260	2203.8	0.998	0.856
141.5	25	150	0.80	0.954	8,711	3910.7	0.996	1.000
43.8	10	50	0.80	0.969	1,214	3518.6	0.997	0.888
43.8	15	150	0.80	0.947	1,615	2687.2	0.997	1.002
88.1	25	150	0.80	0.896	3,913	4616.2	0.996	1.386
23.3	10	150	0.80	0.923	428	2114.2	0.999	1.339
62.5	20	150	0.80	0.896	2,272	4103.8	0.998	1.355
62.5	25	150	0.80	0.923	2,541	4792.2	0.998	1.515
43.8	10	150	0.45	0.799	171	2369.2	1.000	6.309
43.8	20	150	0.80	0.861	1,150	4233.0	0.999	1.876
43.8	25	150	0.80	0.817	1,025	5979.9	0.997	2.631
23.3	15	150	0.80	0.783	285	3721.2	0.998	3.021
23.3	20	150	0.80	0.783	405	4829.2	0.999	2.832
23.3	25	150	0.80	0.637	218	6758.9	0.999	6.594

Q = flow rate (ml/min), L = bed height (cm), C_0 = initial concentration of phenol (ppm), d_p = average particle size (mm), LUB = Equivalent Length of Unused Bed (cm), FLUB = LUB/L, D_L = axial dispersion coefficient (cm²/min), Pe = Peclet number.

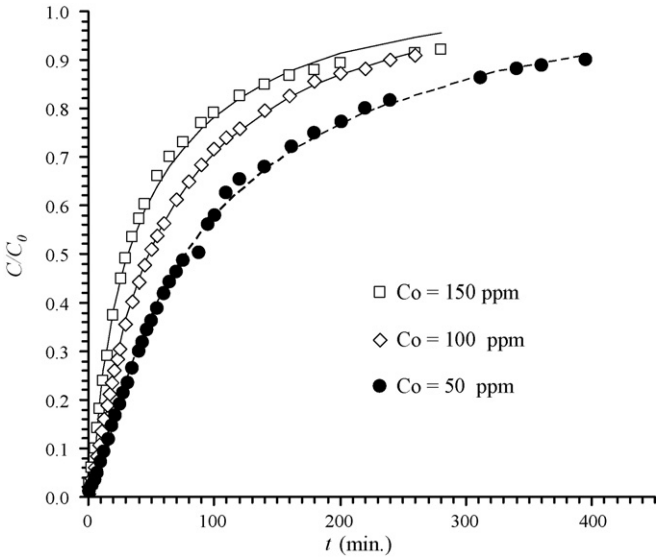

Fig. 6. Effect of initial concentration on breakthrough curves for adsorption of phenol by activated carbon produced from dates' stones. Bed height = 20 cm, d_p = 0.8 mm, and flow rate = 43.8 ml/min.

parameter for the design of an absorber is the Equivalent Length of Unused Bed (LUB), which can be obtained by:

$$\text{LUB} = \left(1 - \frac{W_b}{W_{sat}}\right) L \tag{13}$$

where L is the bed length and W_{sat} is the amount of phenol adsorbed at the saturation of bed. LUB is used to determine the length of a full scale adsorbent bed as the sum of the length of the ideal fixed bed adsorber, i.e. the stoichiometric length of bed needed to produce the desired adsorption capacity of the bed, based on ideal step-function behavior, plus the LUB, as additional length. The LUB Design Approach assumes that the adsorption bed is long enough to produce constant-pattern behavior and that the system is governed by a convex isotherm [47]. Phenol adsorption very well fitted to the Freundlich isotherm, and, therefore, the last assumption is valid for phenol adsorption [5]. Let us define the Fraction Equivalent Length of Unused Bed (FLUB) as:

$$\text{FLUB} = \frac{\text{LUB}}{L} \tag{14}$$

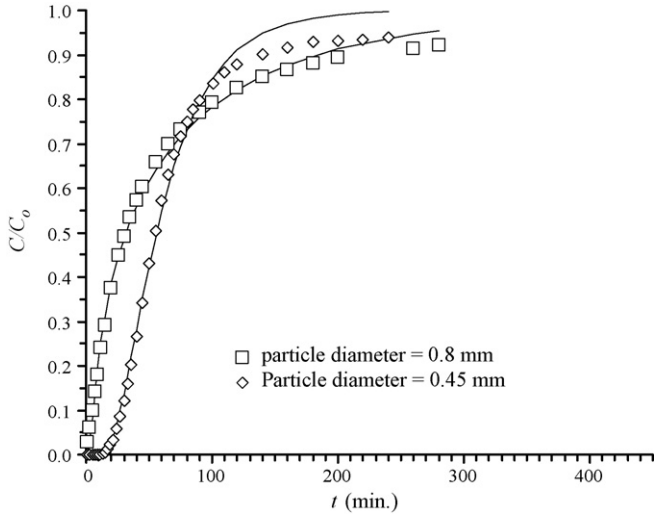

Fig. 7. Effect of particle diameter on breakthrough curves for adsorption of phenol by AC from dates' stones. Bed height = 10 cm, C_0 = 150 ppm, and flow rate = 43.8 ml/min.

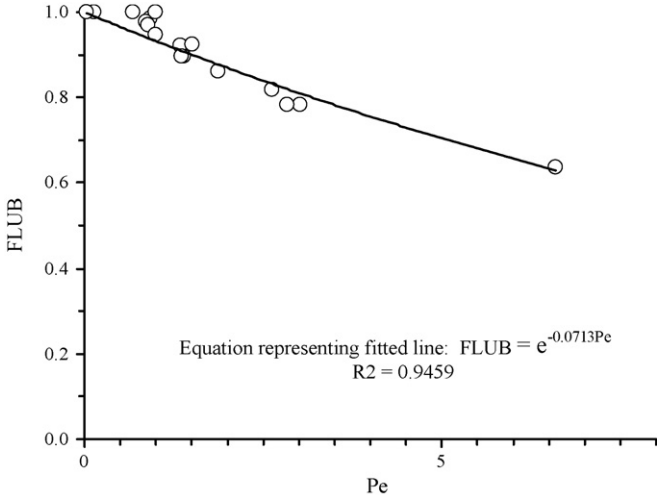

Fig. 8. Fraction of length of unused bed (FLUB) versus *Pe*.

Calculated FLUB from the breakthrough curves and the corresponding *Pe* are also reported in Table 5. When FLUB is plotted versus *Pe* (see Fig. 8), the data were very well correlated with an exponential decay function with R^2 = 0.9459. The resulting expression for the correlation between FLUB and *Pe* is

$$\text{FLUB} = e^{-0.0713(Pe)} \tag{15}$$

Eq. (15) covered the whole range of experimental parameters explored. As *Pe* becomes larger, FLUB decreases exponentially and the adsorption column approach plug flow behavior at very large values of *Pe*. On the other hand when *Pe* = 0, FLUB = 1 and the system becomes a completely mixed. Thus it is clear that Eq. (15) does predict the two limiting values of 1 and 0 for FLUB when *Pe* = 0 and ∞, respectively.

3.2.3. Mass transfer in packed bed adsorber

Assuming that only external film mass transfer is the controlling mechanism during early part of the breakthrough curve and that the rate of mass transfer can be expressed as

$$\frac{\partial q}{\partial t} = k_f a(C - C_i) \tag{16}$$

It is further assumed that $\delta C/\delta t = 0$, and $C_i = 0$; and substituting Eq. (16) into Eq. (9) Eq. (17) is obtained [48]:

$$v\frac{\partial(C)}{\partial z} + \left(\frac{1-\varepsilon}{\varepsilon}\right) k_f a C = D_L \frac{\partial^2 C}{\partial z^2} \tag{17}$$

where k_f is external film mass transfer coefficient, a is external particle surface area per unit volume of particles and C_i interfacial fluid phase solute concentration. Eq. (17) is solved in Ref. [48] with the boundary condition $C = C_0$ at $z = 0$ to give C as function of z, which then can be evaluated at the end of the bed ($z = L$) to give the following expression.

$$\frac{C}{C_0} = \exp\left[\frac{Pe}{2} - \sqrt{\frac{Pe^2}{4} + \frac{(1-\varepsilon)k_f a L^2}{\varepsilon D_L}}\right] \tag{18}$$

Plotting experimental values of C/C_0 versus time, and extrapolating back to $\theta = t/\bar{t} = 1$ (where $\bar{t}$ equal to L/v, is the time required for the first parcel of the solute-rich feed stream to traverse the length of the bed) allows one to determine k_f from Eq. (18) if D_L, v, a, L, and ε are known. The flow rate in the bed must be large enough and/or the bed short enough to generate a nonzero value of C/C_0, in order for this method to work [48]. Breakthrough experimental data satisfying the conditions for the application of Eq. (18) where

Table 6
Comparison between mass transfer coefficients obtained from the analysis of breakthrough curves $(k_f)_{Exp}$ and that obtained from mass transfer correlation $(k_f)_{Corr}$.

Q (ml/min)	L (cm)	C_0 (mg/l)	d_p (mm)	$(k_f)_{Corr}$ (cm/min)	$(k_f)_{Exp}$ (cm/min)	% error
23.9	5	150	1.47	0.233	0.099	57.619
25.6	5	150	0.8	0.313	0.297	5.242
43.8	10	150	0.80	0.427	0.530	−24.207
62.5	15	150	0.80	0.524	0.965	−84.024
43.8	10	100	0.80	0.427	0.735	−72.332
141.5	25	150	0.80	0.847	1.020	−20.402

used to calculate k_f a, using Pe, and D_L obtained from fitting the breakthrough data to Eq. (10) as discussed earlier. For comparison, k_f was calculated using the correlation developed by Wakao and Funazkri [49], which is given by the expression:

$$Sh = 2 + 1.1(\mathrm{Re}_p^{0.6})(Sc^{1/3}) \quad (19)$$

where, Sh and Sc are, respectively, the Sherwood and the Schmidt numbers. The mass transfer area per unit bed volume was calculated as:

$$a = \frac{6(1-\varepsilon)}{d_p} \quad (20)$$

The values of $(k_f)_{Exp}$ calculated using Eq. (18) and those calculated from the mass transfer correlation (Eq. (19)) $(k_f)_{Corr}$, are presented in Table 6 along with relevant experimental conditions. It is seen from Table 6 that for the shortest bed height used (5 cm), excellent agreement between $(k_f)_{Exp}$ and $(k_f)_{Corr}$ is obtained for the smaller particles size (d_p = 0.8). On the other $(k_f)_{Exp}$ was larger than $(k_f)_{Corr}$ for the larger particles size (d_p = 1.47 mm) which can be attributed to a significant contribution of intraparticle diffusion resistance [47,48] due larger d_p. Experiments performed using larger bed heights (10, 15 and 20 cm) gave unacceptably lower values of $(k_f)_{Exp}$ compared and $(k_f)_{Corr}$. This is could be attributed to the violation of the essential condition for application of Eq. (18), that is using small bed height despite the fulfillment of the condition of nonzero condition of C/C_0 in the breakthrough curve [48].

4. Conclusions

It was shown that the adsorption kinetics of phenol on activated carbon (AC) produced from waste dates' stone is very well represented by the pseudo-second order model. The initial rate of adsorption predicted from the pseudo-second order model, decreased with increasing particle diameter (d_p) as a result of higher interfacial area provided by particles with smaller diameter.

Breakthrough curves for phenol removal using a packed bed of activated carbon produced from dates' stones were very well predicted using an axial dispersion model (correlation coefficient 0.997 or better) which enabled the determination of the axial dispersion coefficient and Peclet number (Pe). Analysis of the breakthrough data using the Equivalent Length of Unused Bed (LUB) approach have shown that FLUB (FLUB = LUB/L) is very well correlated with Pe using the relation: $\mathrm{FLUB} = e^{-0.0713(Pe)}$ for the whole range of experimental parameters explored.

Good agreement was found between mass transfer coefficients deduced from the analysis of breakthrough curves and that obtained from correlation available in literature for small particle size and short bed while using larger particle size indicated a significant contribution of intraparticle mass transfer resistance.

Acknowledgments

The research was supported by the Institute of Research and Consultation, King Abdulaziz University, Project No. 115/426. Valuable discussions and comments with Dr. M. Daous at, ChE Dept. KAU are acknowledged.

References

[1] B.S. Girgis, A.A. El-Hendawy, Porosity development in activated carbons obtained from date pits under chemical activation with phosphoric acid, Micropor. Mesopor. Mater. 52 (2002) 105–117.
[2] F. Banat, S. Al-Asheh, L. Al-Makhadmeh, Evaluation of the use of raw and activated date pits as potential adsorbents for dye containing waters, Process Biochem. 39 (2003) 193–202.
[3] N.M. Haimour, S. Emeish, Utilization of dates stones for production of activated carbon using phosphoric acid, Waste Manage. 26 (2006) 651–660.
[4] Y.A. Alhamed, Activated carbon from dates' stones by $ZnCl_2$ activation, JKAU: Eng. Sci. 17 (2006) 75–100.
[5] Y.A. Alhamed, Phenol removal using granular activated carbon from dates' stones, Bulg. Chem. Comm. 41 (2008) 26–35.
[6] Y.A. Alhamed, Phenol removal using granular activated carbon from date's stones by H_3PO_4 activation, J. Env. Prot. Eco. 9 (2008) 417–430.
[7] W.T. Tsai, C.Y. Chang, S.L. Lee, A low cost adsorbent from agricultural waste corn cob by zinc chloride activation, Bioresour. Technol. 64 (1998) 211–217.
[8] W.T. Tsai, C.Y. Chang, S.Y. Wang, C.F. Chang, S.F. Chien, H.F. Sun, Preparation of activated carbons from corn cob catalyzed by potassium salts and subsequent gasification with CO_2, Bioresour. Technol. 78 (2001) 203–208.
[9] C.-F. Chang, C.-Y. Chang, W.-T. Tsai, Effects of burn-off and activation temperature on preparation of activated carbon from corn cob agrowaste by CO_2 and steam, J. Colloid Interface Sci. 232 (2000) 45–49.
[10] W. Qiao, Y. Korai, I. Mochida, Y. Hori, T. Maeda, Preparation of an activated carbon artifact: oxidative modification of coconut shell-based carbon to improve the strength, Carbon 40 (2002) 351–358.
[11] B.S. Girgis, S.S. Yunis, A.M. Soliman, Characteristics of activated carbon from peanut hulls in relation to conditions of preparation, Mater. Lett. 57 (2002) 64–172.
[12] A. Aygun, S. Yenisoy-Karakas, I. Duman, Production of granular activated carbon from fruit stones and nutshells and evaluation of their physical, chemical and adsorption properties, Micropor. Mesopor. Mater. 66 (2003) 189–195.
[13] A.S. Marcilla, M. Garcıa-Garcıa, J. Asensio, A. Conesa, Influence of thermal treatment regime on the density and reactivity of activated carbons from almond shells, Carbon 38 (2000) 429–440.
[14] M. Ahmedna, W.E. Marshall, R.M. Raoa, Production of granular activated carbons from select agricultural by-products and evaluation of their physical, chemical and adsorption properties, Bioresour. Technol. 71 (2000) 113–123.
[15] Z. Hu, E.F. Vansant, Synthesis and characterization of a controlled-microporesize carbonaceous adsorbent produced from walnut shell, Microporous Mater. 3 (1995) 603–612.
[16] K. Gergova, S. Esera, Effects of activation method on the pore structure of activated carbons from apricot stones, Carbon 34 (1996) 879–888.
[17] W. Heschel, E. Klose, On the suitability of agricultural by-products for the manufacture of granular activated carbon, Fuel 74 (1995) 1786–1791.
[18] J. Guo, C. Aik, Lua, Characterization of chars pyrolyzed from oil palm stones for the preparation of activated carbons, J. Anal. Appl. Pyrol. 46 (1998) 113–125.
[19] J. Guo, A.C. Lua, Characterization of chars pyrolyzed from oil palm stones for the preparation of activated carbons, J. Anal. Appl. Pyrol. 46 (1998) 113–125.
[20] A.C. Lua, J. Guo, Preparation and characterization of activated carbons from oil-palm stones for gas-phase adsorption, Colloids Surf. A 179 (2001) 151–162.
[21] J. Guo, A.C. Lua, Textural and chemical characterizations of adsorbent prepared from palm shell by potassium hydroxide impregnation at different stages, J. Colloid Interface Sci. 254 (2002) 227–233.
[22] F. Suarez-Garcıa, A. Martınez-Alonso, J.M.D. Tascon, Pyrolysis of apple pulp: effect of operation conditions and chemical additives, J. Anal. Appl. Pyrol. 62 (2002) 93–109.
[23] F. Suarez-Garcıa, A. Martınez-Alonso, J.M.D. Tascon, Pyrolysis of apple pulp: chemical activation with phosphoric acid, J. Anal. Appl. Pyrol. 63 (2002) 283–301.
[24] J. Hayashi, T. Horikawa, K. Muroyama, V.G. Gomes, Activated carbon from chickpea husk by chemical activation with K_2CO_3: preparation and characterization, Micropor. Mesopor. Mater. 55 (2002) 63–68.
[25] G.H. Oh, C.R. Park, Preparation and characteristics of rice-straw based porous carbons with high adsorption capacity, Fuel 81 (2002) 327–336.
[26] Y. Diao, W.P. Walawender, L.T. Fan, Activated carbon prepared from phosphoric acid activation of grain sorghum, Bioresour. Technol. 81 (2002) 45–52.
[27] A. Bacaoui, A. Yaacoubi, A. Dahbi, C. Bennouna, R. Phan Tan Luu, F.J. Maldonado-Hodar, J. Rivera-Utrilla, C. Moreno-Castilla, Optimization of conditions for the preparation of activated carbons from olive-waste cakes, Carbon 39 (2001) 425–432.

[28] W.K. Lafi, Production of activated carbon from acorns and olive seeds, Biomass Bioenergy 20 (2001) 57–62.
[29] N. Tancredi, N. Medero, F. Moller, J. Piriz, C. Plada, T. Cordero, Phenol adsorption onto powdered and granular activated carbon prepared from Eucalyptus wood, J. Colloid Interface Sci. 279 (2004) 357–363.
[30] http://faostat.fao.org/faostat/form?collection=Production.Crops.Primary&Domain=Production&servlet=1&hasbulk=&version=ext&language=EN.
[31] A. Dabrowski, P. Podkoscielny, Z. Hubicki, M. Barczak, Adsorption of phenolic compounds by activated carbon—a critical review, Chemosphere 58 (2005) 1049–1070.
[32] NOVAWin2, V.2.2, Operation Manual, NOVA Series Windows BASED OPERATING and Data Analysis Software, Quantachrome Instruments, FL, USA, 2006.
[33] S. Lowell, J.E. Shields, M.A. Thomas, M. Thommes, Characterization of Porous Solids and Powders: Surface Area Pore Size and Density, Kluwer Academic Publishers, Netherland, 2004.
[34] X. Yang, B. Al-Duri, Kinetic modeling of liquid-phase adsorption of reactive dyes on activated carbon, J. Colloid Interface Sci. 287 (2005) 25–34.
[35] V.C. Srivastava, M.M. Swamy, I.D. Mall, B. Prasad, I.M. Mishra, Adsorptive removal of phenol by bagasse fly ash and activated carbon: equilibrium, kinetics and thermodynamics, Colloids Surf. A 272 (2006) 89–104.
[36] A.E. Ofomaja, Kinetics and mechanism of methylene blue sorption onto palm kernel fiber, Process Biochem. 42 (2007) 16–24.
[37] S. Lagergren, Zue theorie der sogenannten adsorption gelöster stoffe, vol. 24, Kungliga Svenska Vetenskapsakademiens, Handlingar, 1898, pp. 1–39.
[38] Y.-S. Ho, Citation review of Lagergren kinetic rate equation on adsorption reactions, Scientometrics 59 (2004) 171–177.
[39] B.H. Hameed, A.A. Rahman, Removal of phenol from aqueous solutions by adsorption onto activated carbon prepared from biomass material, J. Hazard. Mater. 160 (2008) 576–581.
[40] Y.S. Ho, G. McKay, A kinetic study of dye sorption by biosorbent waste product pith, Resour. Conserv. Recycl. 25 (1999) 171–193.
[41] A.T. Mohd Din, B.H. Hameed, L. Abdul, Ahmad, Batch adsorption of phenol onto physiochemical-activated coconut shell, J. Hazard. Mater. 161 (2009) 1522–1529.
[42] B.H. Hameeda, M.I. El-Khaiary, Malachite green adsorption by rattan sawdust: isotherm, kinetic and mechanism modeling, J. Hazard. Mater. 159 (2008) 574–579.
[43] A. Kumar, S. Kumar, S. Kumar, D.V. Gupta, Adsorption of phenol and 4-nitrophenol on granular activated carbon in basal salt medium: equilibrium and kinetics, J. Hazard. Mater. 147 (2007) 155–166.
[44] D.O. Cooney, The importance of axial dispersion in liquid phase fixed bed adsorption operations, Chem. Eng. Commun. 110 (1991) 217–231.
[45] L. Lapidus, N.R. Amundsen, Mathematics of adsorption in beds. IV. The effect of longitudinal diffusion in ion exchange and chromatographic columns, J. Phys. Chem. 56 (1952) 984.
[46] M.R. Rosene, Treatment of water by granular activated carbon, in: J.M. McGuire, I.H. Suffet (Eds.), Advances in Chemistry Series 202, American Chemical Society, Washington, DC, 1983, p. 201.
[47] G. Vazquez, R. Alonso, S. Freire, J. Gonzalez-Alvarez, G. Antorrena, Uptake of phenol from aqueous solutions by adsorption, in a *Pinus pinaster* bark packed bed, J. Hazard. Mater. B 133 (2006) 61–67.
[48] D.O. Cooney, Determining external film mass transfer coefficients for adsorption columns, AIChE J. 37 (1991) 1270–1274.
[49] N. Wakao, T. Funazkri, Effect of fluid dispersion coefficient on particle-to-fluid mass transfer coefficients in packed beds correlation of Sherwood numbers, Chem. Eng. Sci. 33 (1978) 1375–1384.